applied sciences

MDPI

Article

Fermented Gold Kiwifruit Protects Mice Against Non-Alcoholic Fatty Liver Disease in a High-Fat Diet Model

Jihye Choi [1], Hwal Choi [1], Yuseong Jang [1], Hyeon-Gi Paik [1], Hyuck-Se Kwon [2] and Jungkee Kwon [1,*]

[1] Department of Laboratory Animal Medicine, College of Veterinary Medicine, Jeonbuk National University, Iksan-si 54596, Jeollabuk-do, Republic of Korea; jyyye@naver.com (J.C.); narcism077@naver.com (H.C.); yuseongjang@naver.com (Y.J.); hyeongipaik@naver.com (H.-G.P.)

[2] R&D Team, Food & Supplement Health Claims, Vitech, #602 Giyeon B/D 141 Anjeon-ro, Iseo-myeon, Wanju-gun 55365, Jeollabuk-do, Republic of Korea; sek2gun@nate.com

* Correspondence: jkwon@jbnu.ac.kr; Tel.: +82-63-850-0951

Abstract: Gold kiwifruit is known for its high vitamin C content and various benefits. This study investigated the effects and molecular mechanisms of fermented gold kiwifruit (FGK) in a mouse model of high-fat diet (HFD)-induced obesity and hepatic steatosis. FGK powder was prepared using five strains of lactic acid bacteria: *L. paracasei*, *Lc. lactis*, *L. acidophilus*, *L. casei*, and *L. helveticus*. ICR mice were fed an HFD for 8 weeks to induce obesity and hepatic steatosis, and FGK supplementation was evaluated for its therapeutic potential. FGK administration significantly reduced serum levels of alanine aminotransferase (ALT), aspartate aminotransferase (AST), total cholesterol, triglyceride, and glucose compared to the HFD-only group. Histopathological analysis showed that FGK reduced lipid accumulation and hepatic lesions, as confirmed by hematoxylin and eosin (H&E) staining. Furthermore, administration of FGK activated the sirtuin 1(SIRT1)/adenosine monophosphate-activated protein kinase (AMPK) pathway and inhibited expression of the pro-inflammatory cytokines such as IL-1β, IL-6, and TNF-α in liver tissue. These findings suggest that FGK could reduce the severity of non-alcoholic fatty liver disease (NAFLD) by inhibiting fat synthesis, promoting fat breakdown, and suppressing inflammation in HFD-induced obese mice.

Keywords: NAFLD; fermented gold kiwifruit; obesity; inflammation; SIRT1/AMPK pathway

Citation: Choi, J.; Choi, H.; Jang, Y.; Paik, H.-G.; Kwon, H.-S.; Kwon, J. Fermented Gold Kiwifruit Protects Mice Against Non-Alcoholic Fatty Liver Disease in a High-Fat Diet Model. *Appl. Sci.* **2024**, *14*, 11503. https://doi.org/10.3390/app142411503

Academic Editors: António José Madeira Nogueira and Andrea Luísa Fernandes Afonso

Received: 8 November 2024
Revised: 5 December 2024
Accepted: 9 December 2024
Published: 10 December 2024

1. Introduction

Non-alcoholic fatty liver disease (NAFLD) is a liver condition defined by the accumulation of more than 5% fat in the liver weight [1]. This condition is primarily associated with metabolic dysfunctions, such as insulin resistance, increased de novo lipogenesis, and reduced fatty acid oxidation [2]. The prevalence of NAFLD has been rapidly increasing in recent years, with significant variations across regions [3]. Studies report that the prevalence of NAFLD is highest in the Middle East (32%) and South America (31%), followed by Asia (27%), North America (24%), and Europe (23%) [4]. The rising prevalence among humans is largely driven by increasing rates of obesity, metabolic syndrome, and sedentary lifestyles worldwide. In contrast to alcohol-induced fatty liver disease, NAFLD develops in individuals with little to no alcohol consumption, and its development is often linked to obesity, type 2 diabetes, and other metabolic disorders [1,2]. NAFLD encompasses a broad spectrum of liver diseases ranging from simple hepatic fat accumulation to non-alcoholic steatohepatitis and hepatocellular carcinoma [5]. It is crucial to manage NAFLD effectively in its early stages to prevent disease progression. However, because of the unclear etiology of NAFLD and its association with various other conditions, there is no established approach for the treatment of NAFLD with proven long-term efficacy [6].

Typically, NAFLD arises due to excessive intracellular lipid accumulation resulting from over-nutrition due to a high-calorie diet [7,8]. As the accumulation of intracellular lipids continues, insulin resistance is induced, leading to inadequate fat breakdown and

elevated delivery of fatty acids to the liver, resulting in the synthesis of new fats. This disruption in normal lipid metabolism initiates cellular stress, inflammasome activation, and eventual cell death [9,10]. The pathogenesis of NAFLD is primarily attributed to liver damage caused by the accumulation of triglycerides (TG) and fatty acids within the liver, and if the condition persists, it may progress to liver fibrosis, eventually contributing to chronic inflammatory processes in other tissue [11]. However, the full etiology of NAFLD remains unclear, and there is currently no established treatment. As dietary control and exercise are considered the best approaches, research on natural substances and drugs that may improve NAFLD is underway [12].

Accumulated TG in liver cells can activate inflammatory pathways such as the nuclear factor of kappa B (NF-κB), contributing to chronic inflammation [13]. Therefore, active suppression of transcription factors for lipid synthesis is a key target in the treatment of NAFLD [14]. Recent studies have revealed that the silent information regulator 1 (SIRT1) and AMP-activated protein kinase (AMPK) pathways are important regulators of lipid and glucose metabolism in hepatic cells, functioning as a vital energy modulator [14,15]. The histone/protein deacetylase SIRT1 is a key factor in the regulation of glucose and lipid metabolism, while AMPK plays a role in various cellular processes, such as lipid metabolism, by inhibiting hepatic fat synthesis and promoting fatty acid oxidation [16,17]. Phosphorylated AMPK (p-AMPK) upregulates the expression of SIRT1, regulates metabolic stress, and contributes to the maintenance of energy homeostasis, especially under conditions of stress or energy depletion [18]. On the other hand, since SIRT1 regulates AMPK activation in the context of NAFLD, a deficiency in SIRT1 leads to a deficiency in AMPK [19]. Thus, targeting the SIRT1/AMPK pathway provides a novel approach to addressing NAFLD and its associated metabolic complications.

Kiwifruit is a crop of high nutritional value, known for its rich content of antioxidants, including vitamin C, vitamin E, and folic acid, along with various biologically active compounds [20]. Historically, the green kiwifruit, primarily known as *Actinidia deliciosa* cv Hayward, has been widely cultivated and was introduced to the market in 1991. In contrast, the gold kiwifruit, referred to as *Actinidia chinensis* cv Hort16A, was developed later and became commercially available in the late 1990s [21]. Gold kiwifruit is recognized for its high content of carotenoids, including lutein and β-carotene, as well as bioactive substances such as quinic acid, caffeic acid, and β-sitosterol [22]. These compounds, along with flavonoids and polyphenols, contribute significantly to its potent antioxidant properties. Gold kiwifruit, in particular, offers a more abundant supply of nutrients like calcium and beta-carotene compared to the more commonly known green kiwifruit [23]. Our previous research demonstrated that fermentation significantly enhances the bioactive compounds in gold kiwifruit, increasing its potential health benefits [24]. Fermented gold kiwifruit has demonstrated efficacy in protecting against acute gastritis and exhibited significant protective effects in models of alcohol-induced liver injury [24,25]. While fermented foods are known to improve metabolic health, limited studies have focused on the effects of fermented gold kiwifruit (FGK) on NAFLD. To the best of our knowledge, this is the first study to investigate the protective effects of FGK on hepatic lipid metabolism and inflammation is an HFD-induced NAFLD model. Consequently, this study aims to evaluate the protective effects of FGK obtained from two strains of lactic acid bacteria isolated from gold kiwifruit peel in mice subjected to a high-fat diet (HFD) to induce non-alcoholic fatty liver disease (NAFLD) and obesity. Furthermore, this study investigated FGK's role in the regulation of hepatic lipid metabolism and inflammation through SIRT1/AMPK signaling pathways in the NAFLD mouse model.

2. Materials and Methods

2.1. Chemical and Regent

Catechin (PHR1963) and Glucose (G7021) were purchased from Sigma-Aldrich (St. Louis, MO, USA). Total cholesterol (TC, BM-CHO-100), High-density lipoprotein (HDL), low-density lipoprotein (LDL)/very-low-density lipoprotein (VLDL) (BM-CHL-100), and TG (BM-TGR-100) were purchased from BIOMAX (Guri, Gyeonggi-do, Republic of Ko-

rea). Primary antibodies such as TNF-α (11948), IL-1β (11242), IL-6 (12912), SIRT1 (8469), AMPK-α (5831), p-AMPK-α (2535), AMPK-β (4150), p-AMPK-β (4186), and β-actin (4970) were purchased from Cell-Signaling Technology (Danvers, MA, USA). Rabbit anti-Goat IgG (H + L)-HRP and Goat anti-mouse IgG (H + L)-HRP antibodies were purchased from GenDEPOT (Katy, TX, USA). TNF-α ELISA kit (MTA00B-1) and IL-6 ELISA kit (M600B) were purchased from R&D System Inc. (Minneapolis, MN, USA). IL-1β ELISA kit (ab197742) was purchased from Abcam (Cambridge, UK).

2.2. Fermented Gold Kiwifruit Powder Preparation

In this study, the FGK was derived from gold kiwifruits cultivated in Jeju, Republic of Korea. The gold kiwifruits were thoroughly washed with distilled water (DW) to eliminate any contaminations, then finely chopped, including the peel. The chopped gold kiwifruit and puree were subjected to fermentation under specific salting and degreasing conditions, following a patented protocol developed by the authors (Patent application number: 10-2474865). After fermentation, the samples were uniformly mixed and inoculated onto Bromocresol Purple (BCP) plate count agar (EIKEN, Japan) and cultured at 37 °C for 48 h. The characteristics of isolated strain were evaluated, resulting in the selection of five lactic acid bacteria strains such as *Lactococcus lactis* VI-01 (KTCT 14351 BP), *Lacticaseibacillus paracasei* VI-02 (KTCT 14352 BP), *Lacticaseibacillus casei* VIGRA01 (KTCT 14756BP), *Lactobacillus helveticus* VICAM05 (KTCT 15949BP), and *Lactobacillus acidophilus* VIFEC24 (KTCT 15950BP). These strains were combined with gold kiwifruit puree in a ratio of 2:8 and subsequently fermented at 37 °C for 8 to 12 h. Following the fermentation, a heat treatment was applied at 90 °C for 30 min to inactivate the bacteria before the concentration and freeze-drying process. The final powder was stored at −70 °C until further use.

2.3. Experimental Animal Model

The experimental design for the animal study was constructed following Li et al. [26]. Male ICR mice weighing 27–29 g were purchased from Damool Sciences (Daejeon, Republic of Korea) and housed at 22 ± 2 °C under a controlled 12-h light/12-h dark cycle (lights on at 8 AM). Animal experiments were approved by the Jeonbuk National University Animal Care Committee (NON2023-044) and performed in accordance with the guidelines for the care and use of animals. The compositions of the normal and high-fat diets are presented in Table 1, and each diet was purchased from Saeronbio Inc. (Uiwang, Gyeonggi-do, Republic of Korea). All animals were acclimatized for one week, and the mice were randomly divided into six groups (n = 6) based on average weight. The six groups were as follows: (1) normal diet (ND) group; (2) high-fat diet (HFD) only group; (3) HFD and oral administration of Catechin 50 mg/kg (Catechin) group; (4) HFD and oral administration of 50 mg/kg of FGK (FGK 50) group; (5) HFD and oral administration of 125 mg/kg FGK (FGK 125) group; (6) HFD and oral administration of 250 mg/kg FGK (FGK 250) group. Catechin and FGK groups were administered to the mice in each group via oral gavage every morning. An equal volume of DW was administered to the ND and HFD groups. Body weight and dietary food intake were monitored twice weekly to track changes in body weight and dietary patterns induced by HFD. The average value per week was recorded. Additionally, body weights were measured the day before autopsy and on the first day, while dietary intake was represented as a daily consumption. After the completion of the 8-week experiment, mice were euthanized via isoflurane (Ifran Liq, Hana Pharm Co., Ltd., Seoul, Republic of Korea) inhalation anesthesia, followed by blood collection. Following blood collection, the mice were euthanized with an additional dose of isoflurane to ensure complete euthanasia. Liver, epididymal fat, and perirenal fat were harvested after mice were confirmed for euthanasia. The organ weights were expressed as weight relative to body weight to account for variations in body weight.

Table 1. Formulations of the normal and high-fat diets.

	High-Fat Diet (HFD)		Normal Diet (ND)	
	g (%)	**kcal (%)**	**g (%)**	**kcal (%)**
Protein	26	20	19.2	20
Carbohydrate	26	20	67.3	70
Fat	35	60	4.3	10
Total		**100**		**100**
kcal/g	5.24		3.85	

g = gram; kcal = kilocalorie.

2.4. Measured of Fasting Blood Glucse and IPGTT

Fasting blood glucose concentrations were assessed at four and eight weeks using a glucometer (Accu-Check Active, Roche Diagnostic GmbH, Mannheim, Germany) in tail vein blood samples obtained following a 12-h fast. During the eight weeks of treatment, an intraperitoneal glucose tolerance test (IPGTT) was performed following a 12-h fast. Blood samples were collected from the mouse tail vein at 30, 60, 90, and 120 min after intraperitoneal administration of glucose (Sigma-Aldrich, St. Louis, Missouri, USA) at 2 g/kg body weight. The area under the curve (AUC) was calculated using the trapezoidal approximation method based on measured blood glucose concentrations. Blood glucose at x minutes was denoted as BG(x), and the AUC was determined as follows [27]:

$$\text{AUC (mg*h/dL)} = \{BG(0) + BG(30)/2\} + \{BG(30) + BG(60)/2\} + \{BG(60) + BG(90)/2\} + \{BG(90) + BG(120)/2\}$$

2.5. Measured of Serum Biochemical Analyses

The blood was collected from centrifuged at 900× *g* at 15 min at 4 °C. The serum was then collected and stored at −70 °C until use. Serum alanine aminotransferase (ALT), aspartate aminotransferase (AST), glucose, and lipase concentrations were performed using a VetTest 8008 chemistry analyzer (IDEXX Laboratories Inc., Westbrook, Cumberland County, ME, USA) on a single VetTest serum biochemistry chip. For the accuracy of the results, VetTest measurements were conducted three times, and the values were summarized as the average values. Serum total cholesterol (TC), triglyceride (TG), and low-density lipoprotein (LDL) and high-density lipoprotein (HDL) levels concentrations were assessed using assay kits (Biomax, Guri, Gyeonggi-do, Republic of Korea). The TC, TG, LDL, and HDL levels were measured using a microplate reader (Synergy 2, BioTek Instrument, Winooski, VT, USA) at 570 nm. All biochemical analyses were performed according to the manufacturer protocols. Detailed protocols are available in the Supplementary Materials.

2.6. Measured of Histopathology Analyses

For histological analysis, harvested liver tissue was fixed in 10% formalin at room temperature with agitation for 24 h. Subsequently, the tissues were embedded in paraffin blocks, cut into 5-µm sections using a microtome, and the sections were mounted on glass slides. The samples on each glass slide were deparaffinized using xylene and graduated alcohol series. Staining was performed using hematoxylin and eosin (H&E). Once staining was complete, the samples were photographed using an optical microscope for analysis of hepatic steatosis. This analysis was conducted following the methodology outlined by Bedossa et al. [28]. The hepatic steatosis scoring parameters are presented in Table 2.

Table 2. Hepatic steatosis scoring scale.

Score	Histological Feature
0	No hepatocytes affected
0.5	Slight damage (0–5%) in liver
1	Mild damage (5–20%) in liver
2	Moderate damage (20–50%) in liver
3	Severe damage (>50%) in liver

2.7. Western Blot Analyses

Proteins from mouse liver were extracted using RIPA buffer containing phosphatase and protease inhibitors. The extracted proteins were quantified using the BCA protein assay (A55864, Thermo Fisher, Middlesex County, MA, USA) and adjusted to equivalent concentrations. Protein separation was performed using 4–20% SDS-page gels, and separated proteins were transferred to a polyvinylidene difluoride (PVDF) membrane (#1620177, Bio-Rad, Contra Costa County, CA, USA). The membrane was blocked at room temperature for 2 h with 5% BSA in PBS-T. After blocking, the membrane was washed with PBS-T and incubated with a primary antibody (Cell-Signaling Technology, Danvers, MA, USA) diluted at 1:1000 in EveryBlot Blocking Buffer (#1201020, Bio-Rad) at 4 °C for 12 h. Following the primary antibody reaction, the membranes were washed with PBS-T, and a second antibody (goat anti-rabbit or goat anti-mouse IgG-HRP, GenDEPOT, Katy, TX, USA) diluted 1:2000 in EveryBlot Blocking Buffer was applied at room temperature for 1 h. After the secondary antibody reaction, the membrane was washed with PBS-T, and the bands were detected using an ECL Western Blotting Substrate kit (#32106, Thermo Fisher, Middlesex County, MA, USA) and analyzed using a Chemi-Imager system (Alpha Immotech, San Leandro, CA, USA). Band intensities were analyzed using the Image J program (NIH, Bethesda, MD, USA), and all bands were normalized to the housekeeping gene (β-actin) before quantification.

2.8. Statistical Analyses

All results are expressed as mean ± SEM and one-way ANOVA was conducted using Prism 9.5 software (GraphPad Software, San Diego, CA, USA) followed by post hoc analysis using Tukey's test. Statistical significance was determined at the $p < 0.05$ level.

3. Results

3.1. Changes in Body Weights and Food Intakes

Figure 1 presents images of the mice and liver image, body weights, food intakes, and organ weights. In the eighth week, mouse body weight measurements were highest in the HFD group (Figure 1C) compared with the ND group but significantly lower body weights in the FGK group. In particular, the FGK 250 group body weights were similar to those in the ND group. Food intake in the ND group was greater than in the other groups (Figure 1D,E), consistent with the results from other studies [29]. Additionally, when comparing relative organ weights at the end of the experiment, the FGK 250 group exhibited lower liver, epididymal, and perirenal fat weights than the HFD group (Figure 1F).

3.2. Fasting Blood Glucose, IPGTT, and AUC

During the experimental period, fasting blood glucose concentrations were measured at four and eight weeks (Figure 2A). At four weeks, significantly higher blood glucose concentrations were measured in the HFD group compared with the ND group ($p < 0.005$). In addition, blood glucose concentrations were also significantly lower in the Catechin and FGK 250 groups. At eight weeks, blood glucose concentrations were significantly elevated in all experimental groups except the FGK 250 group. At eight weeks, we also conducted an intraperitoneal glucose tolerance test (IPGTT) in HFD-induced mice (Figure 2B). The glucose sensitivity in mice fed the HFD was comparable to that in the ND group. At 30 min after the administration of insulin (1 U/kg body weight), an increase in blood glucose concentrations was measured in all groups. Furthermore, compared with the ND group, the HFD groups exhibited significantly higher insulin resistance sensitivity ($p < 0.01$). The increased blood glucose concentrations following insulin administration decreased over time with FGK treatment. In the FGK 250 group, high insulin resistance sensitivity was not evident even 30 min after insulin administration; at 120 min post-insulin administration, blood glucose concentrations were comparable to those of the ND group ($p > 0.05$). The analysis of the area under the curve (AUC) showed an increase in the HFD group and FGK 50 group compared with the ND group (Figure 2C). Additionally, the FGK 250 group

exhibited significantly reduced AUC values compared with the HFD group ($p < 0.01$). These results suggest that the administration of FGK is effective in regulating blood glucose and insulin resistance sensitivity in the context of high-fat diet-induced hyperglycemia, given that blood glucose concentrations in the FGK 250 group were comparable to those of the ND group.

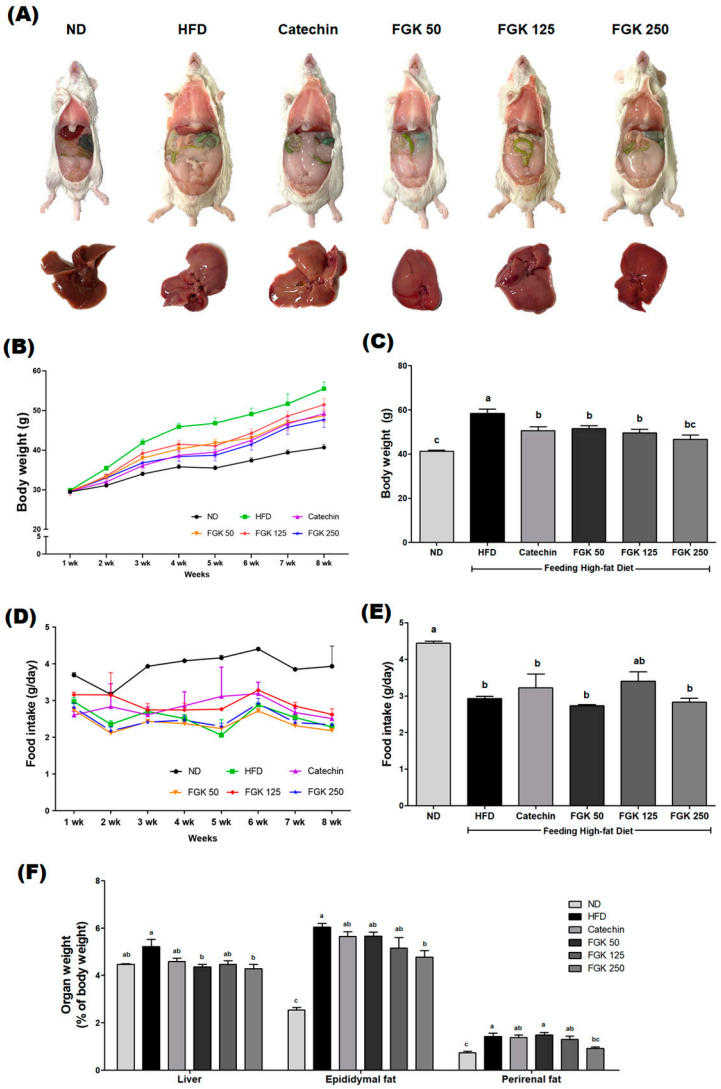

Figure 1. Effects of fermented gold kiwifruit (FGK) on the fat parameters of ICR mice fed with a high-fat diet (HFD): (**A**) representative images of the bodies and livers of mice fed a normal diet (ND) or fed the HFD and administered FGK; (**B**) changes body weight; (**C**) final body weights; (**D**) changes in food intake; (**E**) average daily food intake; and (**F**) relative organ weights. All data are presented as the mean ± SEM ($n = 6$), and different letters (a–c) indicate statistically significant differences between groups at the $p < 0.05$ level using one-way ANOVA analysis after completing post hoc analysis using Tukey's test.

3.3. Serum ALT, AST, Glucose, and Lipase Concentration

First, liver damage was evaluated by examining enzymatic markers (ALT and AST) associated with liver function. The ALT concentrations were significantly increased in the HFD group compared with the ND group (Figure 3A). In the FGK treatment group, a concentration-dependent decrease was observed but was not statistically significant. In the FGK 250 group, ALT concentrations were not significantly different from those in the ND group. Additionally, AST concentrations tended to increase in the HFD group and

decrease in a concentration-dependent manner with FGK administration (Figure 3B), but these findings were not significant ($p > 0.05$).

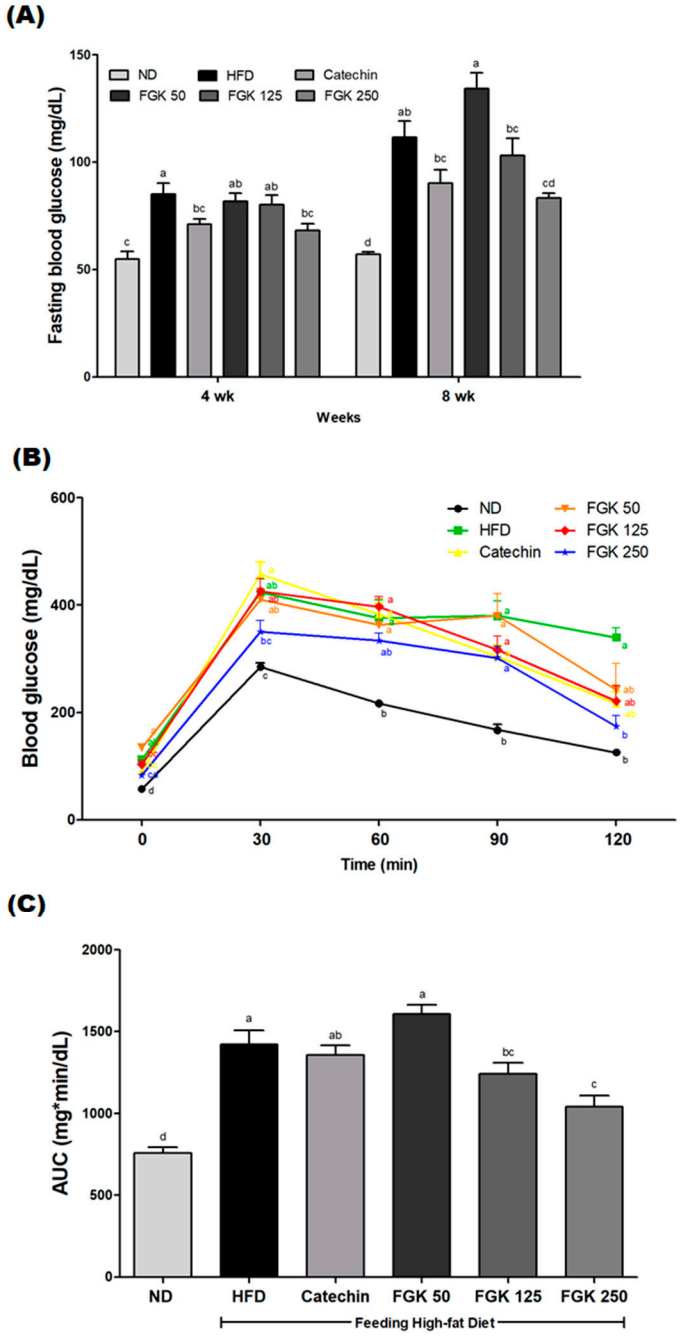

Figure 2. Effects of FGK on the fasting blood concentrations of ICR mice fed with a high-fat diet: (**A**) fasting blood glucose at four and eight weeks; (**B**) IPGTT; (**C**) area under the curve (AUC). All data are presented as the mean ± SEM ($n = 6$), and different letters (a–d) indicate statistically significant differences between groups at the $p < 0.05$ level using one-way ANOVA analysis after completing post hoc analysis using Tukey's test.

Serum glucose concentrations were significantly greater in the HFD group compared with the ND group (Figure 3C). These results indicate similarities with blood glucose levels (Figure 2A), and FGK administration resulted in decreased serum glucose levels as well. In particular, in the FGK 250 group, serum glucose level decreased significantly compared with the HFD group ($p < 0.05$). Additionally, serum lipase concentrations were higher in

the HFD group compared with the ND group (Figure 3D), while the FGK administration group exhibited serum lipase concentrations similar to the ND group.

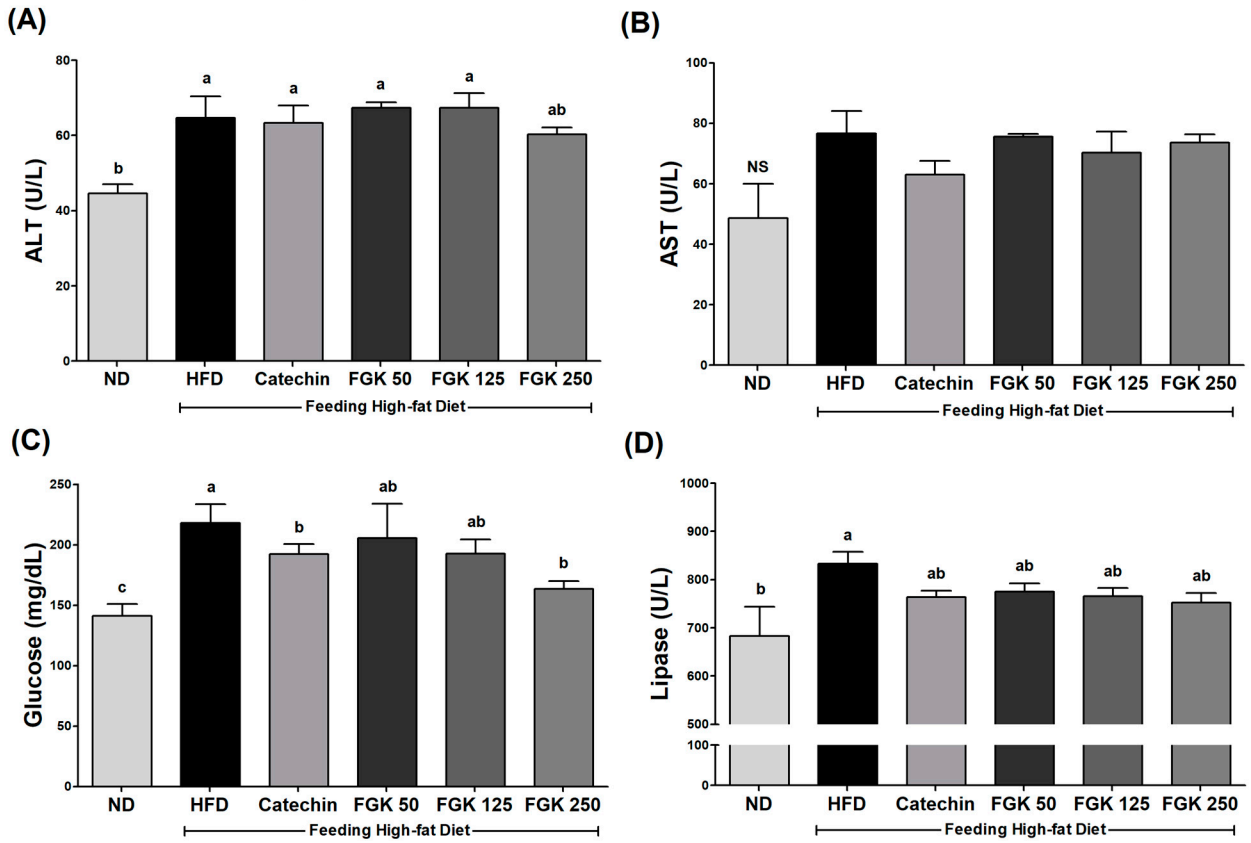

Figure 3. Effects of FGK on serum (**A**) ALT, (**B**) AST, (**C**) glucose, and (**D**) lipase concentration of ICR mice fed with a high-fat diet. All data are presented as the mean ± SEM (n = 6), and different letters (a–c) indicate statistically significant differences between groups at the $p < 0.05$ level using one-way ANOVA analysis after completing post hoc analysis using Tukey's test, while NS indicates no significant difference.

3.4. Serum Lipid Profile

Several studies have indicated that feeding laboratory animals an HFD leads to increased serum TC, TG, and LDL concentrations and decreased serum HDL concentrations. In this study, serum TC, TG, and LDL concentrations were significantly higher in the HFD group (Figure 4A–C), while HDL was significantly lower than the ND group (Figure 4D). These results indicate the success of the NAFLD mouse model. In the FGK administration group, serum TC, TG, and LDL concentrations were reduced and HDL concentrations increased in a dose-dependent manner compared with the HFD group.

3.5. Histological Examination of Liver Tissue

To determine the scores for hepatic steatosis, this study performed histopathological examinations of the liver tissues of all experimental groups (Figure 5). In comparison with the ND group, the liver tissues from the HFD group exhibited more severe steatosis, with an elevated average score of 2.8 ± 0.2 (Figure 5B). The presence of intracellular lipid droplets in the Catechin group led to a score of 2.2 ± 0.2. Although mild to severe hepatic steatosis was present in the FGK 50, 125, and 250 groups, the steatosis scores of 1.5 ± 0.2, 1.4 ± 0.2, and 0.9 ± 0.1, respectively, indicate a gradual dose-dependent reduction.

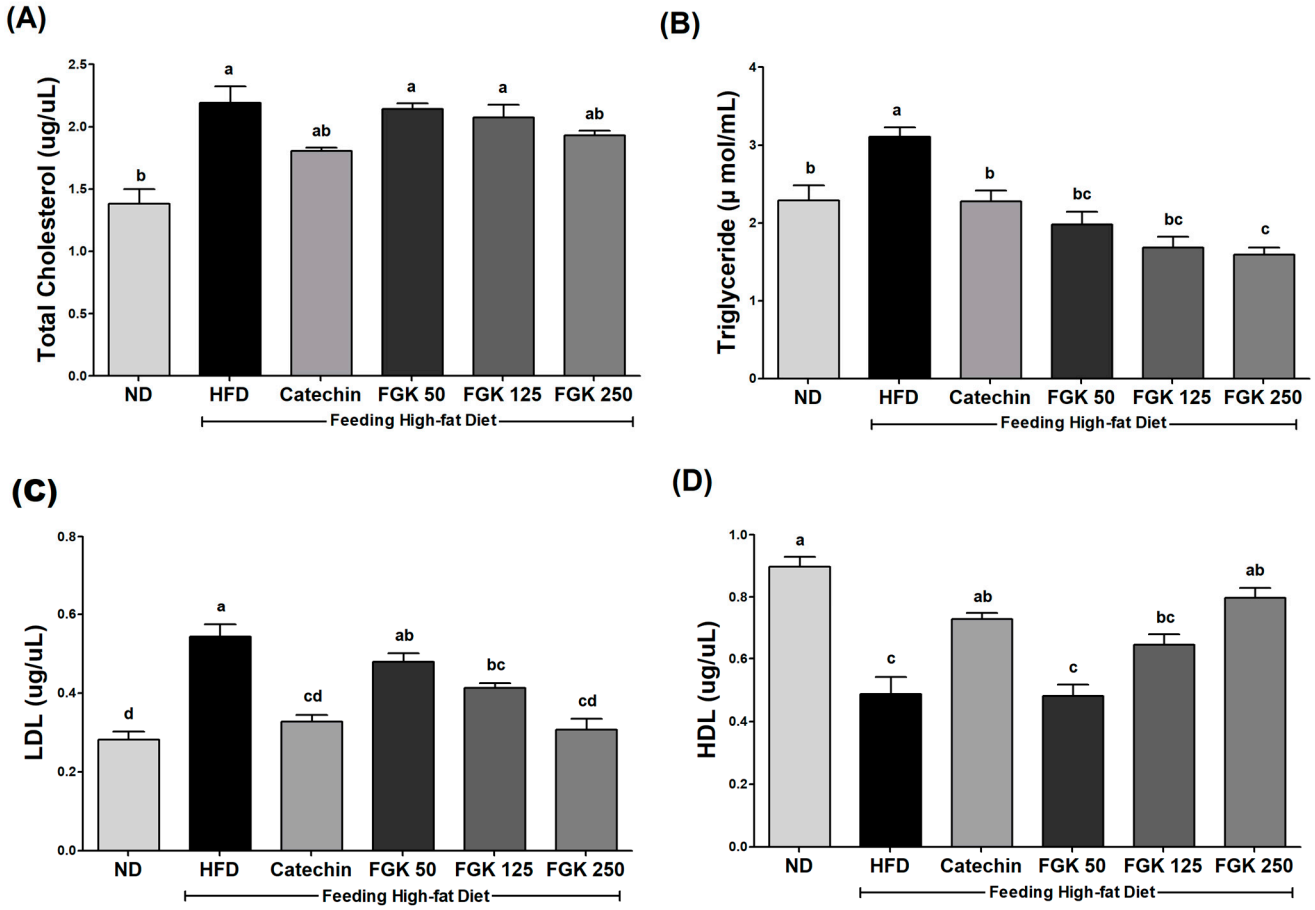

Figure 4. Effects of FGK on serum lipid profile levels of ICR mice fed with a high-fat diet: (**A**) total cholesterol (TC); (**B**) triglyceride (TG); (**C**) low-density lipoprotein (LDL); (**D**) high-density lipoprotein (HDL). All data are presented as the mean ± SEM (n = 6), and different letters (a–d) indicate statistically significant differences between groups at the $p < 0.05$ level using one-way ANOVA analysis after completing post hoc analysis using Tukey's test.

3.6. Effects of Serum Cytokine Levels

This study performed serum cytokine analysis to evaluate the effects of FGK administration on inflammation induced by HFD. Serum TNF-α showed a 47.98% increase in the HFD group (376.6 ± 6.1 pg/mL) compared with the ND group (256.5 ± 8.9 pg/mL), respectively, which decreased in a dose-dependent manner due to FGK administration (Figure 6A). In the FGK 250 group (263.1 ± 5.2 pg/mL), a 44.28% decrease in TNF-α concentration compared with the HFD group was observed. Serum IL-1β increased by 25.03% in the HFD group (8.99 ± 1.0 pg/mL) compared with the ND group (7.19 ± 0.2 pg/mL, Figure 6B). This serum IL-1β concentration showed a significant decrease compared with the HFD group in the Catechin group (7.67 ± 0.1 pg/mL) and the FGK 250 group (7.23 ± 0.1 pg/mL, $p < 0.05$). Additionally, serum IL-6 concentration results showed a significant increase in the HFD group, 68.6 ± 8.3 pg/mL, compared with the ND group, 32.9 ± 3.1 pg/mL ($p < 0.05$). These increased values showed a dose-dependent decrease in the FGK administration groups, with values of 41.5 ± 3.2 pg/mL, 38.1 ± 2.4 pg/mL, and 32.2 ± 3.2 pg/mL, respectively (Figure 6C).

3.7. Expression of Hepatic Inflammatory Cytokines

The expression of hepatic inflammatory factors in response to NAFLD development and the inhibitory effects of FGK. In our study, the expression of TNF-α, IL-1β, and IL-6 increased in the HFD group (Figure 7), while inflammatory cytokine expression was

reduced by FGK administration in a dose-dependent manner. Therefore, we discovered that FGK administration in mice fed an HFD contributes to the suppression of fat generation and a decrease in inflammatory factors.

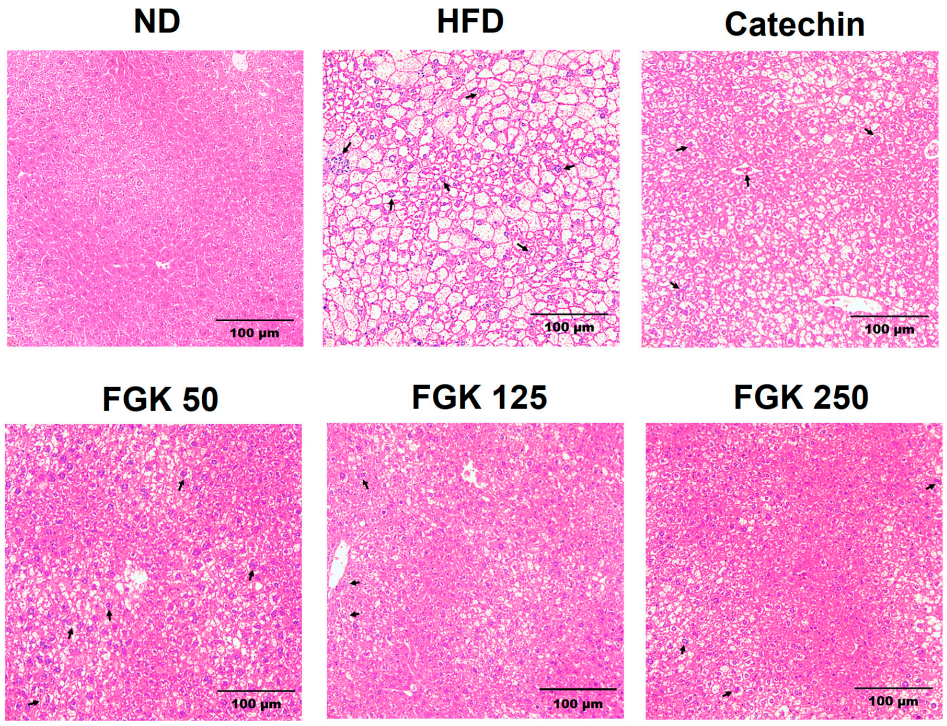

(**A**)

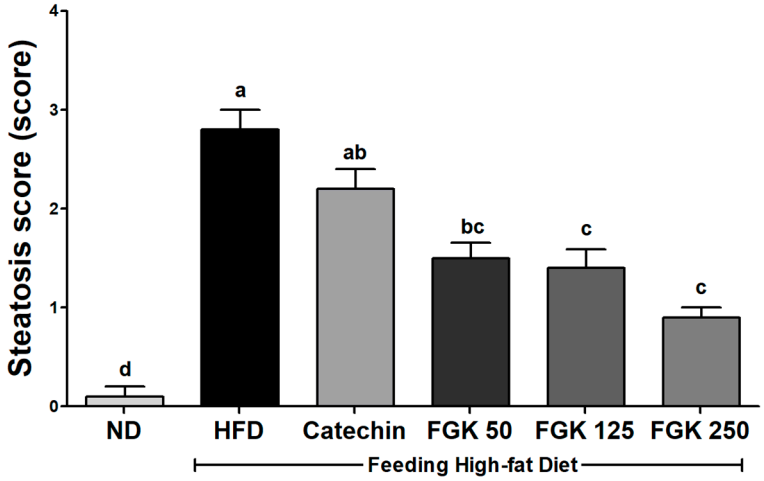

(**B**)

Figure 5. Effects of FGK on the livers of ICR mice fed with a high-fat diet: (**A**) H&E-stained hepatic tissue sections (×400). Rats induced with HFD exhibited hepatocellular steatosis characterized by intracellular lipid droplets with clear vacuoles indicative of fatty changes (black arrows); (**B**) steatosis score. All data are presented as the mean ± SEM ($n = 6$), and different letters (a–d) indicate statistically significant differences between groups at the $p < 0.05$ level using one-way ANOVA analysis after completing post hoc analysis using Tukey's test.

3.8. Expression of Hepatic SIRT1/AMPK Pathway

Based on previously reported results in hepatic steatosis studies, our goal was to investigate whether FGK administration could impact the SIRT1/AMPK pathway. A marked reduction in SIRT1 expression was detected in the HFD group (Figure 8). This

decreased expression was restored in a dose-dependent manner in FGK groups. To assess the involvement of AMPK activation and assessed the expression of AMPK-α and –β. While activation of AMPK-α was not detected in the Catechin group, FGK administration led to its restored activity compared to the ND group. Moreover, AMPK-β demonstrated dose-dependent activation with FGK administration. Therefore, FGK administration led to the improvement of NAFLD through the SIRT1/AMPK pathway.

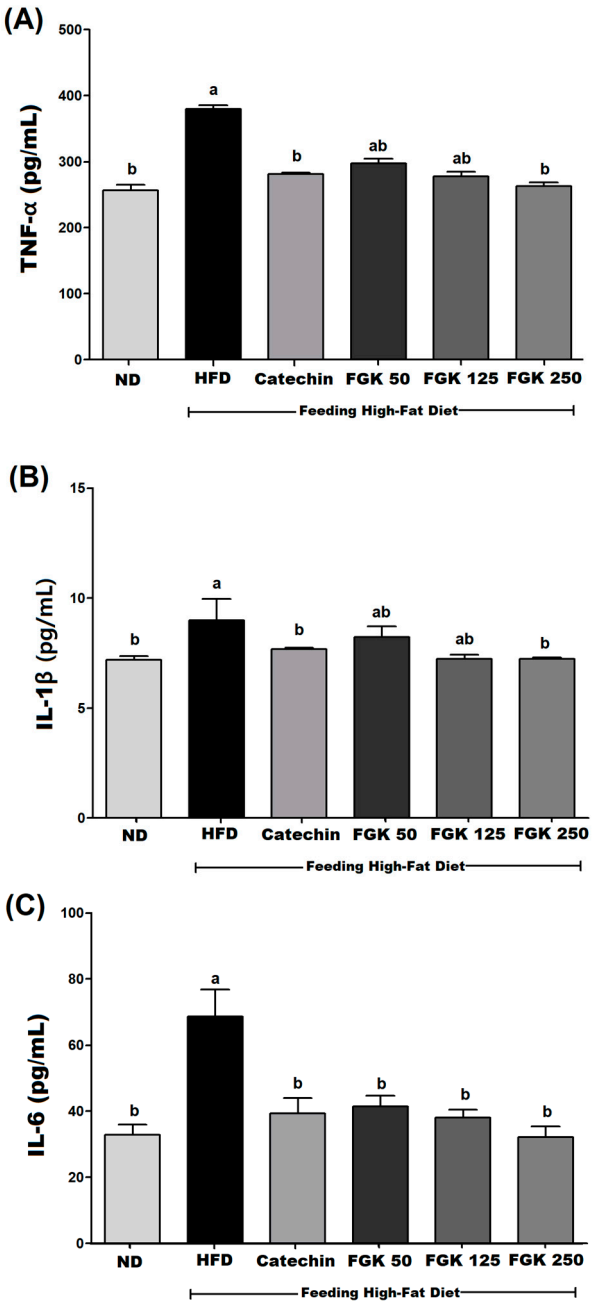

Figure 6. Effects of FGK on the serum cytokines concentration of ICR mice fed with a high-fat diet; (**A**) Serum TNF-α concentration; (**B**) Serum IL-1β concentration; (**C**) Serum IL-6 concentration. All data are presented as the mean ± SEM ($n = 6$), and different letters (a,b) indicate statistically significant differences between groups at the $p < 0.05$ level using one-way ANOVA analysis after completing post hoc analysis using Tukey's test.

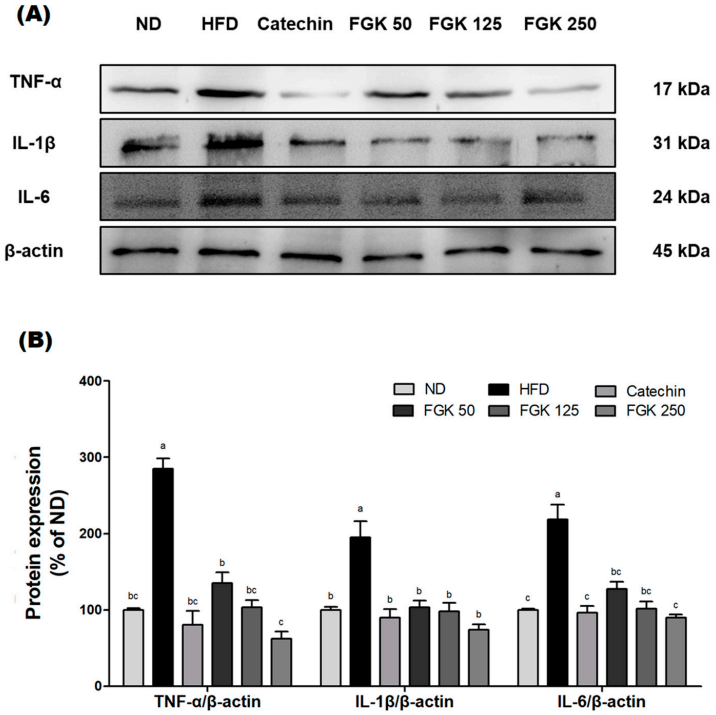

Figure 7. Effects of FGK on hepatic expression of inflammatory cytokines in ICR mice fed with a high-fat diet. (**A**) protein expression image; (**B**) relative optical density as measured using Image J (Java 1.8.0) software. All data are presented as the mean ± SEM (n = 6), and different letters (a–c) indicate statistically significant differences between groups at the $p < 0.05$ level using one-way ANOVA analysis after completing post hoc analysis using Tukey's test.

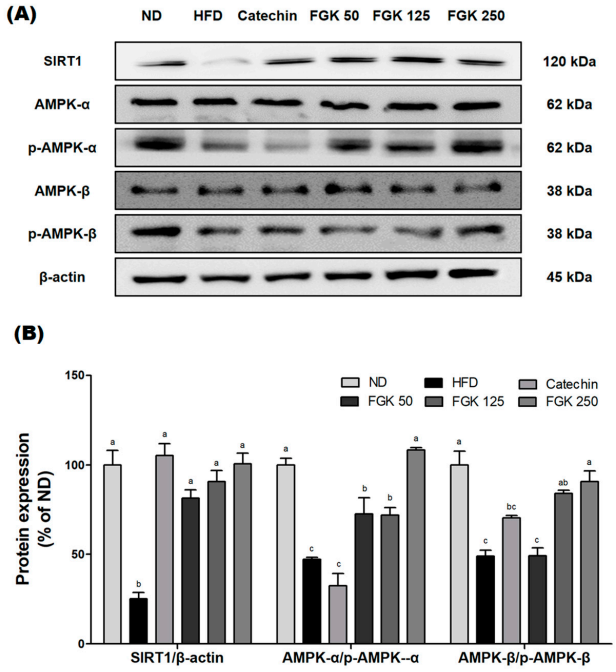

Figure 8. Effects of FGK on hepatic expression of SIRT1/AMPK pathway proteins in ICR mice fed with a high-fat diet; (**A**) protein expression image; (**B**) relative optical density as measured using Image J software. All data are presented as the mean ± SEM (n = 6), and different letters (a–c) indicate statistically significant differences at the $p < 0.05$ level after completing post hoc analyses using Tukey's test.

4. Discussion

This study demonstrated the beneficial effects of FGK administration on metabolic syndrome and inflammation in HFD-induced NAFLD mice. Our results showed that FGK significantly reduced the levels of serum ALT, AST, TC, TG, and glucose, indicating its protective effects against NAFLD-related liver damage and metabolic dysfunction. Furthermore, FGK inhibited the expression of inflammatory factors through the SIRT1/AMPK pathway, which plays a central role in lipid metabolism, oxidative stress, and inflammation regulation. The SIRT1/AMPK pathway is known to play a crucial role in the occurrence of metabolic syndrome and inflammation related to NAFLD, as well as oxidative stress.

The administration of a high-fat diet (HFD) with elevated fat content is a well-established model for inducing obesity and NAFLD in mice by providing a high-calorie intake [30]. In this study, HFD-fed mice exhibited insulin resistance (IR), as confirmed by our IPGTT analysis, and hepatic steatosis, as observed in H&E-stained liver sections. These findings align with previous studies demonstrating that the HFD induces metabolic dysfunction, including impaired glucose metabolism and lipid accumulation in the liver [31]. FGK administration, however, significantly improved glucose tolerance and reduced hepatic lesions, suggesting its potential to mitigate NAFLD progression. NAFLD development is closely linked to excessive lipid accumulation, which leads to mitochondrial dysfunction, hepatocyte apoptosis, and inflammatory response [30,31]. Our results demonstrated that FGK administration reduced serum ALT and AST levels, indicating its hepatoprotective effects in HFD-fed mice. This aligns with the proposed role of antioxidants and bioactive compounds in fermented foods, which have been reported to improve liver function [24]. Furthermore, similar to finding in other studies, FGK administration reduced serum TC and TG concentrations and improved lipid metabolism in NAFLD models. These effects are likely mediated through the inhibition of de novo lipogenesis (DNL), a process that contributes to TG accumulation and is considered a therapeutic target in metabolic disorders [31]. AMPK, a key regulator of lipid and glucose metabolism, has been highlighted in recent studies as a critical pathway for addressing metabolic disorders, including NAFLD [32,33]. In this study, FGK activated the SIRT1/AMPK pathway, which is known to reduce lipid synthesis and promote fatty acid oxidation. This provides a mechanistic basis for the observed improvements in lipid metabolism and inflammation, further justifying FGK's potential as a therapeutic agent.

AMPK is a key regulator of protein that plays important roles in aging, inflammation, oxidative stress, and lipid and glucose metabolism [34]. Its activation is crucial for mitigating hepatic steatosis in NAFLD, as it reduces lipid markers such as TG and LDL while promoting fatty acid oxidation [35]. Similarly, SIRT1 is a transcription factor known as the "master regulator of metabolism", playing a central role in lipid metabolism homeostasis by regulating processes such as lipid accumulation and maturation in hepatic lipid metabolism and inflammation [32,36]. Together, SIRT1 and AMPK regulate lipid metabolism through mutual interaction, forming a vital axis in addressing metabolic disorders. Several studies have reported that activation of the SIRT1/AMPK pathway in mice with NAFLD is associated with the alleviation of hepatic steatosis, inhibition of oxidative stress, and protection against metabolic disorders [13,37]. In our study, FGK administration activated and upregulated the SIRT1/AMPK pathway, as demonstrated by reduced hepatic steatosis and inflammation in HFD-fed mice. These findings suggest that FGK's bioactive compounds, enhanced through fermentation, may directly modulate this pathway to exert its protective effects against NAFLD. In addition, factors such as lipopolysaccharide (LPS) and inflammatory cytokines such as TNF-α increase in patients with NAFLD, leading to decreased AMPK activity [38,39]. Our results demonstrated that FGK suppressed the expression of these inflammatory mediators, further contributing to the restoration of AMPK activity and energy homeostasis. Therefore, regulation of inflammatory factors in the context of NAFLD is a key area for future research to understand the mechanisms governing hepatic AMPK activity [40].

The inflammatory response is another important factor influencing the onset and course of NAFLD [41]. Chronic inflammation not only exacerbates insulin resistance but also contributes to hepatic steatosis and fibrosis, which are key features of NAFLD. Pro-inflammatory cytokines such as the IL-1 family (IL-1F) and TNF-α play significant roles in the regulation of inflammation-related insulin resistance [42,43]. Specifically, TNF-α contributes to the development of hepatic steatosis and IR in NAFLD and plays a critical role in metabolic inflammation by regulating the inflammatory process in the liver [43]. Metabolic inflammation, a hallmark of disorders such as obesity, type 2 diabetes, and NAFLD, is primarily driven by excessive nutrient intake, particularly dietary lipids [44].

Lipotoxicity, as manifested here, primarily occurs in organs involved in lipid metabolism, such as the liver, muscle, and adipose tissue. In particular, the degree of adipose tissue inflammation strongly correlates with the severity of liver inflammation in NAFLD [45]. Similarly, IL-1β is a critical mediator in hepatic inflammatory processes, influencing insulin resistance and fibrosis [43]. IL-1β acts through specific receptors and is characterized by a short half-life [46]. In particular, IL-1β is known to activate the nucleotide-binding and oligomerization domain-like receptor family (NLR) pyrin-domain-containing (NLRP) 3 inflammasome, which is implicated in the onset of type 2 diabetes [47]. In addition, IL-6 appears to be synthesized in response to liver damage, regulates the liver damage/regeneration process, and promotes insulin resistance, which impairs glucose homeostasis [48]. Our study discovered that the consumption of FGK suppresses the expression of inflammatory cytokines induced by high-calorie and high-fat diets. The anti-inflammatory activity of FGK observed in this study is similar to the results observed in our previous study on alcoholic liver injury [23]. Therefore, this study hypothesizes that the administration of FGK may contribute to the alleviation of NAFLD through the inhibition of inflammation.

When these results are considered together, the fermentation process enhanced the bioactive compounds in kiwifruit, such as flavonoids and carotenoids, which exhibited significant anti-inflammatory and antioxidant effects [24,25]. These enhanced compounds contributed to the improvement of HFD-induced NAFLD mice. In our HFD model, NAFLD is characterized by hyperlipidemia and hepatic steatosis, similar to NAFLD in humans. Mice fed an HFD and administered FGK showed significantly lower blood glucose levels and reduced weight gain, suggesting that FGK mitigates metabolic dysfunction associated with HFD consumption. The results also indicated a reduction of insulin resistance, as demonstrated by reductions in ALT and AST biomarkers that are associated with liver damage. FGK also modulated lipid metabolism by reducing TC, TG, and LDL levels, while increasing HDL levels, while increasing HDL levels, indicating its potential to improve overall lipid profiles in NAFLD models. Furthermore, in mice fed the HFD, FGK also appeared to activate the SIRT1/AMPK pathway in the liver, effectively inhibiting factors of activated inflammatory cytokines (Figure 9). These dual mechanisms—modulating lipid metabolism and suppressing inflammation—highlight FGK's unique therapeutic in addressing the complex pathophysiology of NAFLD. These findings suggest that FGK may have beneficial pharmacological effects in HFD-induced hepatic steatosis and insulin resistance.

Together, the results indicate that FGK influenced the regulation of hepatic lipid metabolism by reducing lipid synthesis and insulin resistance. This study hypothesizes that these effects occurred through activation of the SIRT1/AMPK pathway. Consequently, our study results indicate the potential therapeutic utility of FGK as a novel SIRT1/AMPK activator for the treatment of NAFLD. In addition, this study also anticipates that FGK administration may prevent the progression from NAFLD to non-alcoholic steatohepatitis (NASH) by suppressing liver inflammation; however, additional research is needed to further elucidate the molecular mechanisms and effects of FGK.

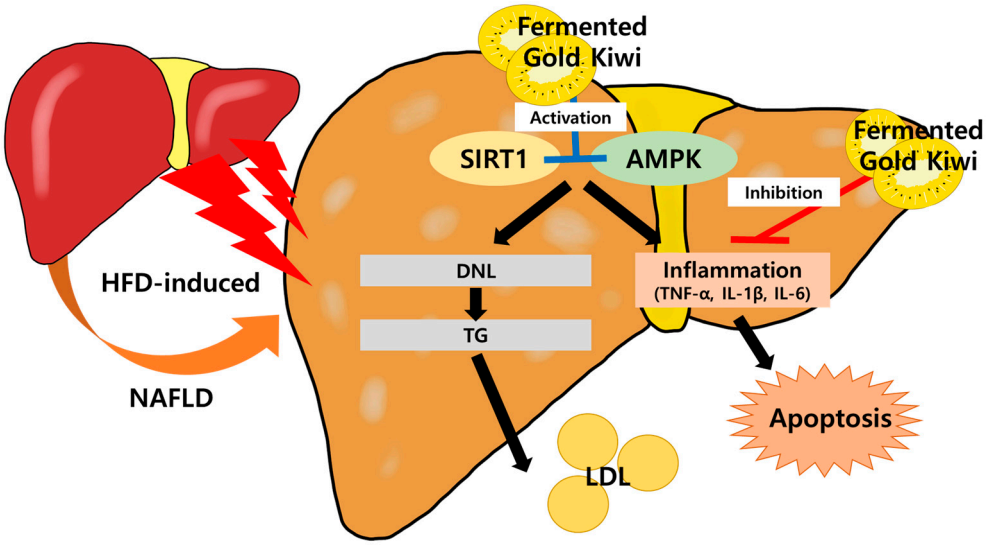

Figure 9. Illustration of SIRT1/AMPK pathway activation by FGK and the inhibitory of FGK on NAFLD in mice. The blue line represents the activation of the SIRT1/AMPK pathway, while the red line indicates the inhibition of inflammation by FGK. Each black arrow signifies the progression to the next step in the pathway. HFD, high-fat diet; SIRT1, sirtuin 1; AMPK, AMP-activated protein kinase; DNL, de novo lipogenesis; TG, triglyceride; LDL, low-density lipoprotein; TNF-α, tumor necrosis factor α; IL-1β, interleukin 1 β; IL-6, interleukin 6.

5. Conclusions

In conclusion, this study demonstrated that FGK administration effectively mitigates the elevation of blood glucose concentrations and insulin resistance induced by an HFD, therefore ameliorating NAFLD in a mouse model. These effects were closely associated with the activation of the SIRT1/AMPK pathway, which not only improved hepatic lipid metabolism but also suppressed hepatic inflammation. Additionally, FGK administration demonstrated potential in preventing NAFLD progression by targeting key metabolic and inflammatory pathways. Despite these promising findings, the study did not investigate the specific metabolites resulting from the fermentation process that could be contributing to these effects. Understanding these metabolites and their mechanisms would provide a deeper insight into FGK's role in modulating inflammation and lipid metabolism. Future studies could focus on metabolite profiling to elucidate these pathways further. Taken together, these findings highlight the pharmacological potential of FGK as a dietary intervention for NAFLD and provide a foundation for further research into its mechanisms and clinical applications.

Supplementary Materials: The following supporting information can be downloaded at: https://www.mdpi.com/article/10.3390/app142411503/s1.

Author Contributions: Conceptualization, J.C. and J.K.; methodology, J.C. and H.C.; validation, J.C., H.C., Y.J. and H.-G.P.; formal analysis, J.C.; investigation, J.C. and H.C.; resources, H.-S.K.; data curation, J.C.; writing—original draft preparation, J.C.; writing—review and editing, J.C. and J.K.; visualization, J.C.; supervision, H.-S.K. and J.K.; project administration, H.-S.K. and J.K. All authors have read and agreed to the published version of the manuscript.

Funding: This research received no external funding.

Institutional Review Board Statement: The animal study protocol was approved by the Ethics Committee of Jeonbuk National University (protocol code NON2023-044 and date of 02 March 2023).

Informed Consent Statement: Not applicable.

Data Availability Statement: The data presented in this study are available on request from the corresponding author (Jungkee Kwon). The data are not publicly available due to ethical restrictions.

Conflicts of Interest: Authors Jihye Choi, Hwal Choi, Yuseong Jang, Hyeon-Gi Paik, and Jungkee Kwon are employed by the Jeonbuk National University. Hyuck-Se Kwon is employed by the company Vitech Co., Ltd. The remaining authors declare that the research was conducted in the absence of any commercial or financial relationships that could be construed as a potential conflict of interest.

Abbreviations

High-fat diet (HFD); Non-alcoholic fatty liver disease (NAFLD); Fermented gold kiwifruit (FGK); Hematoxylin and eosin (H&E); Alanine aminotransferase (ALT); Aspartate aminotransferase (AST); Total cholesterol (TC); Triglyceride (TG); Silent information regulator transcript-1 (SIRT1); Adenosine monophosphate-activated protein kinase (AMPK); Interleukin-1β (IL-1β); Interleukin-6 (IL-6); Tumor necrosis factor-α (TNF-α); Nuclear factor of kappa B (NF-κB); Normal diet (ND); Intraperitoneal glucose tolerance test (IPGTT); The area under the curve (AUC); Low-density lipoprotein (LDL); High-density lipoprotein (HDL); De novo lipogenesis (DNL).

References

1. Recena Aydos, L.; Aparecida do Amaral, L.; Serafim de Souza, R.; Jacobowski, A.C.; Freitas Dos Santos, E.; Rodrigues Macedo, M.L. Nonalcoholic fatty liver disease induced by high-fat diet in C57bl/6 models. *Nutrients* **2019**, *11*, 3067. [CrossRef]
2. Santos, H.O.; Penha-Silva, N. Revisiting the concepts of de novo lipogenesis to understand the conversion of carbohydrates into fats: Stop overvaluing and extrapolating the renowned phrase "fat burns in the flame of carbohydrate". *Nutrition* **2024**, *130*, 112617. [CrossRef]
3. Eng, J.M.; Estall, J.L. Diet-induced models of non-alcoholic fatty liver disease: Food for thought on sugar, fat, and cholesterol. *Cells* **2021**, *10*, 1805. [CrossRef]
4. Younossi, Z.; Anstee, Q.M.; Marietti, M.; Hardy, T.; Henry, L.; Eslam, M.; George, J.; Bugianesi, E. Global burden of NAFLD and NASH: Trends, predictions, risk factors and prevention. *Nat. Rev. Gastroenterol. Hepatol.* **2018**, *15*, 11–20. [CrossRef]
5. Huang, W.C.; Xu, J.W.; Li, S.; Ng, X.E.; Tung, Y.T. Effects of exercise on high-fat diet-induced non-alcoholic fatty liver disease and lipid metabolism in ApoE knockout mice. *Nutr. Metab.* **2022**, *19*, 10. [CrossRef]
6. Friedman, S.L.; Neuschwander-Tetri, B.A.; Rinella, M.; Sanyal, A.J. Mechanisms of NAFLD development and therapeutic strategies. *Nat. Med.* **2018**, *24*, 908–922. [CrossRef]
7. Buzzetti, E.; Pinzani, M.; Tsochatzis, E.A. The multiple-hit pathogenesis of non-alcoholic fatty liver disease (NAFLD). *Metabolism* **2016**, *65*, 1038–1048. [CrossRef]
8. Tung, Y.-T.; Zeng, J.-L.; Ho, S.-T.; Xu, J.-W.; Li, S.; Wu, J.-H. Anti-NAFLD Effect of Djulis Hull and Its Major Compound, Rutin, in Mice with High-Fat Diet (HFD)-Induced Obesity. *Antioxidants* **2021**, *10*, 1694. [CrossRef]
9. Sanyal, A.J. Past, present and future perspective in nonalcoholic fatty liver disease. *Nat. Res. Gastroenterol. Hepatol.* **2019**, *16*, 377–386. [CrossRef]
10. Powell, E.E.; Wong, V.W.; Rinella, M. Non-alcoholic fatty liver disease. *Lancet* **2021**, *397*, 2212–2224. [CrossRef]
11. Zhou, Y.; Ding, Y.L.; Zhang, J.L.; Zhang, P.; Wang, J.Q.; Li, Z.H. Alpinetin improved high fat diet-induced non-alcoholic fatty liver disease (NAFLD) through improving oxidative stress, inflammatory response and lipid metabolism. *Biomed. Pharmacother.* **2018**, *97*, 1397–1408. [CrossRef]
12. Lonardo, A.; Arab, J.P.; Arrese, M. Perspectives on precision medicine approaches to NAFLD diagnosis and management. *Adv. Ther.* **2021**, *38*, 2130–2158. [CrossRef]
13. Li, C.X.; Gao, J.G.; Wan, X.Y.; Chen, Y.; Xu, C.F.; Feng, Z.M.; Zeng, H.; Li, Y.M.; Ma, H.; Xu, P.; et al. Allyl isothiocyanate ameliorates lipid accumulation and inflammation in nonalcoholic fatty liver disease via the Sirt1/AMPK and NF-κB signaling pathways. *World J. Gastroenterol.* **2019**, *25*, 5120–5133. [CrossRef]
14. Lioi, C.J.; Lee, Y.K.; Ting, N.C.; Chen, Y.L.; Shen, S.C.; Wu, S.J.; Huang, W.C. Protective effects of licochalcone A amliorates obesity and non-alcoholic fatty liver diesase via promotion of the Sirt-1/AMPK pathway in mice fed a high-fat diet. *Cells* **2019**, *8*, 447. [CrossRef]
15. Miller, R.A.; Brinbaum, M.J. An energetic tale of AMPK-independent effects of metformin. *J. Clin. Investig.* **2010**, *120*, 2267–2270. [CrossRef]
16. Zhu, Y.; Liu, R.; Shen, Z.; Cai, G. Combination of luteolin and lycopene effectively protect against the "two-hit" in NAFLD through Sirt1/AMPK signal pathway. *Life Sci.* **2020**, *256*, 117990. [CrossRef]
17. Herzig, S.; Shaw, R.J. AMPK: Guardian of metabolism and mitochondrial homeostasis. *Nat. Rev. Mol. Cell Biol.* **2018**, *19*, 121–135. [CrossRef]
18. Mei, Y.; Hu, H.; Deng, L.; Sun, X.; Tan, W. Therapeutic effects of isosteviol sodium on non-alcoholic fatty liver disease by regulating autophagy via Sirt1/AMPK pathway. *Sci. Rep.* **2022**, *12*, 12857. [CrossRef]

19. Liou, C.J.; Wei, C.H.; Chen, Y.L.; Cheng, C.Y.; Wang, C.L.; Huang, W.C. Fisetin Protects Against Hepatic Steatosis Through Regulation of the Sirt1/AMPK and Fatty Acid β-Oxidation Signaling Pathway in High-Fat Diet-Induced Obese Mice. *Cell Physiol. Biochem.* **2018**, *49*, 1870–1884. [CrossRef]
20. Richardson, D.P.; Ansell, J.; Drummond, L.N. The nutritional and health attributes of kiwifruit: A review. *Eur. J. Nutr.* **2018**, *57*, 2659–2676. [CrossRef]
21. Bublin, M.; Mari, A.; Ebner, C.; Knulst, A.; Scheiner, O.; Hoffmann-Sommergruber, K.; Breiteneder, H.; Radauer, C. IgE sensitization profiles toward green and gold kiwifruit differ among patients allergic to kiwifruit from 3 European countries. *J. Allergy Clin. Immunol.* **2004**, *114*, 1169–1175. [CrossRef]
22. Lippi, G.; Mattiuzzi, C. Kiwifruit and cancer: An overview of biological evidence. *Nutr. Cancer* **2020**, *72*, 547–553. [CrossRef]
23. Sivakumaran, S.; Huffman, L.; Sivakumaran, S.; Drummond, L. The nutritional composition of Zespri® SunGold Kiwifruit and Zespri® Sweet Green Kiwifruit. *Food Chem.* **2018**, *238*, 195–202. [CrossRef]
24. Jeon, E.-J.; Choi, J.-H.; Lee, N.-Y.; Oh, H.-J.; Kwon, H.-S.; Kwon, J. Gastroprotective Effects of Fermented Gold Kiwi (*Actinidia chinenesis* L.) Extracts on HCl/EtOH-Induced Gastric Injury in Rats. *Appl. Sci.* **2022**, *12*, 5271. [CrossRef]
25. Choi, J.; Lee, S.; Choi, H.; Lee, J.; Lee, N.; Oh, H.; Kwon, H.; Kwon, J. Fermented gold kiwi prevents and attenuates chronic alcohol-induced liver injury in mice via suppression of inflammatory responses. *Appl. Sci.* **2023**, *13*, 1877. [CrossRef]
26. Li, J.; Wu, H.; Liu, Y.; Yang, L. High fat diet induced obesity model using four strains of mice: Kunming, C57BL/6m BALB/c and ICR. *Exp. Anim.* **2020**, *69*, 326–335. [CrossRef]
27. Choi, J.H.; Kim, S.H.; Lee, E.B.; Kim, J.S.; Jung, J.E.; Jeong, U.Y.; Kim, J.H.; Jang, H.H.; Park, S.Y.; Kim, G.C.; et al. Anti-Diabetic Effects of *Allium hookeri* Extracts Prepared by Different Methods in Type 2 C57BL/J-*db*/*db* Mice. *Pharmaceuticals* **2022**, *15*, 486. [CrossRef]
28. Bedossa, P.; Poynard, T. An algorithm for the grading of activity in chronic hepatitis C. The METAVIR Cooperative Study Group. *Hepatology* **1996**, *24*, 289–293. [CrossRef]
29. Ren, S.M.; Zhang, Q.Z.; Chen, M.L.; Jiang, M.; Zhou, Y.; Xu, X.J.; Wang, D.M.; Pan, Y.N.; Liu, X.Q. Anti-NAFLD effect of defatted walnut powder extract in high fat diet-induced C57BL/6 mice by modulating the gut microbiota. *J. Ethnopharmacol.* **2021**, *270*, 113814. [CrossRef]
30. Im, Y.R.; Hunter, H.; de Gracia Hahn, D.; Duret, A.; Cheah, Q.; Dong, J.; Fairey, M.; Hjalmarsson, C.; Li, A.; Lim, H.K.; et al. A systemic review of animal models of NAFLD finds high-fat, high-fructose diet most closely resenble human NAFLD. *Hepatology* **2021**, *74*, 1884–1901. [CrossRef]
31. Lian, C.Y.; Zhai, Z.Z.; Li, Z.F.; Wang, L. High fat diet-triggered non-alcoholic fatty liver disease: A review of proposed mechanisms. *Chem. Biol. Interact.* **2020**, *330*, 109199. [CrossRef]
32. Anggreini, P.; Kuncoro, H.; Sumiwi, S.A.; Levita, J. Role of the AMPK/SIRT1 pathway in non-alcoholic fatty liver disease (Review). *Mol. Med. Rep.* **2023**, *27*, 35. [CrossRef]
33. von Loeffelholz, C.; Coldewey, S.M.; Birkenfeld, A.L. A Narrative Review on the Role of AMPK on De Novo Lipogenesis in Non-Alcoholic Fatty Liver Disease: Evidence from Human Studies. *Cells* **2021**, *10*, 1822. [CrossRef]
34. Jeon, S.M. Regulation and functional of AMPK in physiology and diseases. *Exp. Mol. Med.* **2016**, *48*, e245. [CrossRef]
35. Fouqueray, P.; Bolze, S.; Dubourg, J.; Hallakou-Bozec, S.; Theurey, P.; Grouin, J.M.; Chevalier, C.; Gluais-Dagorn, P.; Moller, D.E.; Cusi, K. Pharmacodynamic effects of direct AMP kinase activation in humans with insulin resistance and non-alcoholic fatty liver disease: A phase 1b study. *Cell Rep. Med.* **2021**, *2*, 100474. [CrossRef]
36. Schug, T.T.; Li, X. Sirtuin 1 in lipid metabolism and obesity. *Ann. Med.* **2011**, *43*, 198–211. [CrossRef]
37. Li, N.; Yin, L.; Shang, J.; Liang, M.; Liu, Z.; Yang, H.; Qiang, G.; Du, G.; Yang, X. Kaempferol attenuates nonalcoholic fatty liver disease in type 2 diabetic mice via the SirT1/AMPK signaling pathway. *Biomed. Pharmacother.* **2023**, *165*, 115113. [CrossRef]
38. Steinberg, G.R.; Michell, B.J.; van Denderen, B.J.; Watt, M.J.; Carey, A.L.; Fam, B.C.; Andrikopoulos, S.; Proietto, J.; Görgün, C.Z.; Carling, D.; et al. Tumor necrosis factor alpha-induced skeletal muscle insulin resistance involves suppression of AMP-kinase signaling. *Cell Metab.* **2006**, *4*, 465–474. [CrossRef]
39. Galic, S.; Fullerton, M.D.; Schertzer, J.D.; Sikkema, S.; Marcinko, K.; Walkley, C.R.; Izon, D.; Honeyman, J.; Chen, Z.P.; van Denderen, B.J.; et al. Hematopoietic AMPK β1 reduces mouse adipose tissue macrophage inflammation and insulin resistance in obesity. *J. Clin. Investig.* **2011**, *121*, 4903–4915. [CrossRef]
40. Smith, B.K.; Marcinko, K.; Desjardins, E.M.; Lally, J.S.; Ford, R.J.; Steinberg, G.R. Treatment of nonalcoholic fatty liver disease: Role of AMPK. *Am. J. Physiol. Endocrinol. Metab.* **2016**, *311*, E730–E740. [CrossRef]
41. Duarte, M.; Coelho, I.C.; Patarrão, R.S.; Almeida, J.I.; Penha-Gonçalves, C.; Macedo, M.P. How Inflammation Impinges on NAFLD: A Role for Kupffer Cells. *Biomed. Res. Int.* **2015**, *2015*, 984578. [CrossRef]
42. Donath, M.Y.; Shoelson, S.E. Type 2 diabetes as an inflammatory disease. *Nat. Rev. Immunol.* **2011**, *11*, 98–107. [CrossRef]
43. Niederreiteer, L.; Tilg, H. Cytokines and fatty liver disease. *Liver Res.* **2018**, *2*, 14–20. [CrossRef]
44. Tilg, H.; Zmora, N.; Adolph, T.E.; Elinav, E. The intestinal microbita fuelling metabolic inflammation. *Nat. Res. Immunol.* **2020**, *20*, 40–54. [CrossRef]
45. du Plessis, J.; van Pelt, J.; Korf, H.; Mathieu, C.; van der Schueren, B.; Lannoo, M.; Oyen, T.; Topal, B.; Fetter, G.; Nayler, S.; et al. Association of adipose tissue inflammation with histologic severity of nonalcoholic fatty liver disease. *Gastroenterology* **2015**, *149*, 635–648. [CrossRef]

46. Donath, M.Y.; Böni-Schnetzler, M.; Ellingsgaard, H.; Halban, P.A.; Ehses, J.A. Cytokines production by islets in health and diabetes: Cellular origin, regulation and function. *Trends Endocrinol. Metab.* **2010**, *21*, 261–267. [CrossRef]
47. Schroder, K.; Zhou, R.; Tschopp, J. The NLRP3 inflammasome: A sensor for metabolic danger? *Sciences* **2010**, *327*, 296–300. [CrossRef]
48. Skuratovskaia, D.; Komar, A.; Vulf, M.; Quang, H.V.; Shunkin, E.; Volkova, L.; Gazatova, N.; Zatolokin, P.; Litvinova, L. IL-6 Reduces Mitochondrial Replication, and IL-6 Receptors Reduce Chronic Inflammation in NAFLD and Type 2 Diabetes. *Int. J. Mol. Sci.* **2021**, *22*, 1774. [CrossRef]